Journal of The Electrochemical Society, **161** (1) A194-A200 (2014)
0013-4651/2014/161(1)/A194/7/$31.00 © The Electrochemical Society

Propylene Carbonate (PC)-Based Electrolytes with High Coulombic Efficiency for Lithium-Ion Batteries

Hui Zhao, Sang-Jae Park, Feifei Shi, Yanbo Fu, Vincent Battaglia,* Philip N. Ross, Jr.,* and Gao Liu*,z

Lawrence Berkeley National Laboratory, Berkeley, California 94720, USA

A homologous series of propylene carbonate (PC) analog solvents with increasing length of linear alkyl substitutes were synthesized and used as co-solvents with PC for graphite-based lithium-ion half cells. A graphite anode reaches a capacity of around 310 mAh/g in PC and its analog co-solvents, with 99.95 percent Coulombic efficiency, similar to the values obtained with ethylene carbonate-based electrolytes. Solvent interaction with the graphite anode and subsequent decomposition determines the graphite anode performance. Gaseous products from cyclic carbonates with short alkyl chains cause exfoliation of the graphite anode; solvents with longer alkyl chains are able to prevent graphite exfoliation when used as co-solvents with PC. The PC co-solvents compete for solvation of the Li ion with the PC solvent, delaying PC co-intercalation. Reduction products of PC on a graphite surface via a single-electron path form a stable Solid Electrolyte Interphase (SEI), which allows the reversible cycling of graphite.
 [DOI: 10.1149/2.095401jes]

Manuscript submitted July 22, 2013; revised manuscript received November 11, 2013. Published December 10, 2013.

As an important candidate for an electric vehicle (EV) and hybrid electric vehicle (HEV) power source, lithium-ion batteries based on a graphite anode and an ethylene carbonate (EC)-containing electrolyte can be used for a variety of applications. Ethylene carbonate forms a stable solid electrolyte interphase (SEI) at ∼0.8 V before lithium intercalation. Being Li^+ permeable and electronically non-conductive, SEI prevents further electrolyte decomposition and allows reversible lithiation and delithiation of the graphite anode.[1] The major disadvantage of EC is its high melting point at around 34°C, since EC is a solid material at room temperature it needs other co-solvents such as dimethyl carbonate (DMC) and diethyl carbonate (DEC) to be a liquid electrolyte. The relatively high melting point of EC also limits the use of lithium-ion batteries at low temperatures. Propylene carbonate (PC), in contrast, has a wide liquid temperature range (−48.8 ∼ 242.0°C) and very good low-temperature performance when compared to EC.[2] However, with only a negligible structural difference from EC, PC undergoes a detrimental solvent decomposition on the surface of graphite with high crystallinity. This causes disintegration of the graphite electrode, usually accompanied by delamination of the active material from the current collector, and finally, cell failure.

Two different theories are commonly used to explain the detrimental effect of PC in a graphite lithium-ion battery. In the first scenario originally proposed by Peled and developed by Aurbach,[3] the decomposition voltage of the cyclic carbonates is at 0.8 ∼ 1.0 V. This value is higher than the lithium intercalation voltage (0.01 ∼ 0.25 V). The decomposition products form a surface film (SEI), which is compact and protective in the case of EC, preventing further solvent co-intercalation into graphene layers. However, the surface film formed by the PC is not so effective, thus solvent co-intercalation occurs and the resulting decomposition products cause deterioration of the graphite capacity and reversibility. Besenhard and Winter[1,4] proposed the formation of solvated graphite-intercalation compounds (GICs)-$Li(solv)_yC_n$. Co-intercalation of solvents and the subsequent decomposition products determine the cell behavior.

Based on Besenhard and Winter's solvent co-intercalation theory, the model in Figure 1 is used to explain graphite exfoliation in the PC. The dots represent Li^+, and the circles represent PC molecules. For illustration, this model assumes a solvation number of 2, although a more realistic value is about 3 or 4.[5] When using pure PC as a solvent, as presented in Figure 1, solvated Li^+ tend to drag PC molecules into graphene layers in the process of intercalation. There are a lot of electrons in the graphite in the discharge (lithiation) process, which cause a two-electron reduction of the PC. As shown in Figure 1, each PC molecule consumes two electrons and decomposes to lithium carbonate (Li_2CO_3) and propene. The propene gas induces microcracks inside the graphite particles, which lead to disintegration of the graphite electrode. Formation of graphite-intercalation compounds (GICs) was detected by X-ray measurement.[6] Yamada et al. showed that PC exfoliation is prevented by changing PC/DMC ratio from 1/1 to 1/7, the lack of a PC molecule in the Li^+ solvation sheath contributes to this behavior.[7] Cresce et al. recently used mass spectroscopy with a soft ionization technique electrospray ionization to study the Li^+ solvation structure,[8,9] which revealed a close connection between the SEI component and Li^+ solvation structure. Chung et al. modified different parameters that could influence the solvent decomposition behavior in a graphite half cell,[10] the overall results show how solvent co-intercalation affects the cell performance.

We took a different approach to studying the origin of graphite exfoliation. In this work, a homologous series of PC derivatives with increasing length of linear alkyl substitutes were synthesized and used as co-solvents for graphite lithium-ion half cells. Following Besenhard and Winter's concept that the initial stage of electrolyte reduction on graphite proceeds through a co-intercalated state, replacing the PC in the inner solvation sphere of lithium with homologous molecules having progressively longer alkyl chains might have two effects on the chemistry of electrolyte reduction: (1) changing the molecular weight of reduction products so that gas formation may not be observed, thus the problem of graphite exfoliation can be addressed with larger molecular weight; and (2) a steric hindrance to co-intercalation without excessively altering the electrochemical potential or kinetics of reduction and allowing for reduction products to form on the external surface of the graphite and reducing exfoliation. Both effects were observed in this work, which further confirms the effectiveness of Besenhard and Winter's model.

Experimental

All reagents used to synthesize the cyclic carbonates were purchased from Sigma-Aldrich or TCI America and used without further purification. Battery-grade lithium hexafluorophosphate ($LiPF_6$) was purchased from BASF. A Celgard 3501 Separator membrane was a gracious gift from Celgard. Battery-grade acetylene black (AB) was obtained from Denka Singapore Private Ltd, the PVDF KF1100 binder was acquired from Kureha, Japan. The graphite used in this work is CGP-G8, which was obtained from ConocoPhillips. Coin cells were prepared with lithium metal as counter electrode. The slurry preparation, electrode coating, and cell fabrication can be found in the literature.[11]

The cyclic carbonates were synthesized based on a literature procedure.[12] Products were purified by vacuum distillation and dried using 4 Å molecular sieves. A Mettler Toledo DL39 Karl Fisher

*Electrochemical Society Active Member.
zE-mail: gliu@lbl.gov

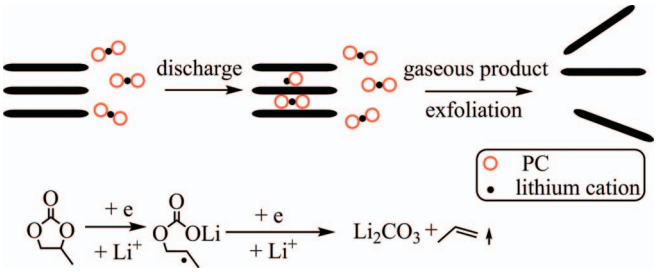

Figure 1. The proposed two-electron reduction path of PC when co-intercalated into graphite in the discharge (lithiation) process, assuming a solvation number of 2.

Coulometer was used to monitor the water content to be less than 30 parts per million (ppm) before it was used.

A Bruker Biospin Advance II 500 MHz NMR spectrometer was used to collect the proton and carbon nuclear magnetic resonance (NMR) spectra of the synthesized products. The NMR spectra are shown in the supporting information (Figure S1 to Figure S10).

Butylene carbonate (BuC): ^{1}H NMR (500 MHz, $CDCl_3$), δ 4.71 (tt, 1H), 4.52 (dd, 1H), 4.09 (dd, 1H), 1.79 (m, 2H), 1.02 (t, 3H), ^{13}C NMR (500 MHz, $CDCl_3$), δ 155.6, 77.1, 69.1, 31.9, 14.5.

Pentylene carbonate (PeC): ^{1}H NMR (500 MHz, $CDCl_3$), δ 4.71 (tt, 1H), 4.52 (dd, 1H), 4.09 (dd, 1H), 1.83 (m, 1H), 1.68 (m, 1H), 1.50 (m, 1H), 1.43 (m, 1H), 0.98 (t, 3H), ^{13}C NMR (500 MHz, $CDCl_3$), δ 155.6, 77.3, 69.2, 36.2, 17.9, 13.2.

Hexylene carbonate (HeC): ^{1}H NMR (500 MHz, $CDCl_3$), δ 4.71 (tt, 1H), 4.52 (dd, 1H), 4.09 (dd, 1H), 1.84 (m, 1H), 1.70 (m, 1H), 1.49 (tt, 2H), 1.38 (m, 2H), 0.93 (t, 3H), ^{13}C NMR (500 MHz, $CDCl_3$), δ 155.6, 77.2, 68.8, 33.4, 26.2, 21.2, 14.2.

Octylene carbonate (OcC): ^{1}H NMR (500 MHz, $CDCl_3$), δ 4.71 (tt, 1H), 4.52 (dd, 1H), 4.09 (dd, 1H), 1.83 (m, 1H), 1.70 (m, 1H), 1.48 (m, 1H), 1.38 (m, 1H), 1.36 ~ 1.22 (m, 6H), 0.92 (t, 3H), ^{13}C NMR (500 MHz, $CDCl_3$), δ 155.6, 77.5, 69.3, 34.4, 31.8, 29.3, 25.3, 22.7, 14.1.

Dodecylene carbonate (DoC): ^{1}H NMR (500 MHz, $CDCl_3$), δ 4.71 (tt, 1H), 4.52 (dd, 1H), 4.09 (dd, 1H), 1.84 (m, 1H), 1.71 (m, 1H), 1.48 (m, 1H), 1.18 (m, 1H), 1.38~1.20 (m, 14H), 0.88 (t, 3H), ^{13}C NMR (500 MHz, $CDCl_3$), δ 155.6, 77.2, 69.2, 34.2, 31.0, 29.8, 29.6, 29.5, 24.4, 22.8, 14.6.

The ionic conductivity of the cyclic carbonates with 1 M $LiPF_6$ was measured using a sample cell constructed of stainless steel disks separated by a Teflon collar, containing a sample 0.61 cm in radius and 0.0156 cm in thickness. Electro-impedance Spectroscopy was used the measure the conductivity, on a VMP galvanostat/potentiostat (Bio-Logic). The sample cell containing electrolytes was brought to 10 mV before impedance measurement was taken in the range from 0.05 Hz to 1 MHz.

Morphology of the electrode surface was characterized using a JSM-7500F scanning electron microscopy (SEM). Attenuated Total Reflectance (ATR) mode FTIR spectra were recorded using Thermo-nexus 670 directly on the electrodes' surfaces. After cycling, the graphite electrodes were washed with dimethyl carbonate (DMC) solvent to remove residual electrolyte inside the argon filled glove box. A homemade transfer system, equipped with a gate valve and a magnetic manipulator, was used to transfer the highly sensitive samples from the pure argon atmosphere of the glove box to the SEM and ATR-IR system.

Results and Discussion

Synthesis and characterization of the mono-substituted cyclic carbonates.— The mono-substituted cyclic carbonates were synthesized from commercial mono-substituted epoxides with different chain lengths (Figure 2). Chromium salen complexes were used to catalyze the reaction between carbon dioxide and expoxides, based on a literature procedure.[12] Products with smaller substituents such as butylene carbonate (BuC), pentylene carbonate (PeC), and hexylene carbonate (HeC) were obtained with high yield (> 95%). Generation of bulky cyclic carbonates such as octylene carbonate (OcC) and dodecylene carbonate (DoC) leads to an increase of the viscosity in the reaction mixture, yields are only 80 percent for OcC and 65 percent for DoC.

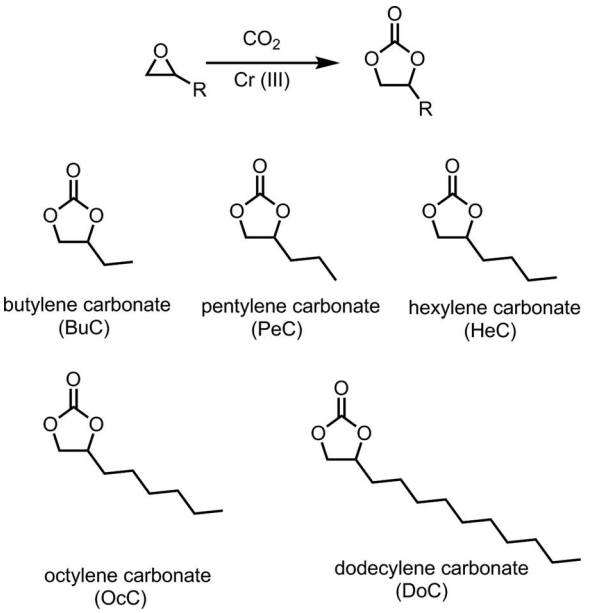

Figure 2. Synthesis of a series of cyclic carbonate derivatives.

Table I shows the ionic conductivities of the synthesized solvents. The conductivities decrease for the electrolytes with solvents that have longer alkyl chains. Solvents with longer chain length have a lower dielectric constant and higher viscosity, both leading to lower conductivity.

Solvents cause graphite exfoliation (BuC and PeC).— CGP-C8 graphite was used to assemble a lithium-ion half cell. A Celgard 3501 separator is well-wetted by PC and all the synthesized cyclic carbonates. When graphite half cells cycle in BuC or PeC, the voltage curves never drop to the lithium intercalation region. Instead, the voltage curves only stop at around 0.6 to 1.2 V corresponds to the continuous decomposition on the graphite surface (Figure 3). This plateau occurs at 0.6 V for PeC, compared to BuC (1.0 V) and PC

Table I. The ionic conductivities of the electrolytes based on the synthesized cyclic carbonates.

Cyclic carbonates	Conductivity of 1 M $LiPF_6$ in different cyclic carbonate solvents at 30°C (mS/cm)
PC	5.1
BuC	3.1
PeC	2.3
HeC	0.5
HeC/PC = 4[a]	2.3
OcC	0.4
OcC/PC = 2[a]	1.9
DoC[b]	X
DoC/PC = 1[a]	1.2

[a]volume ratio.
[b]DoC is a solid material at room temperature, conductivity is not characterized.

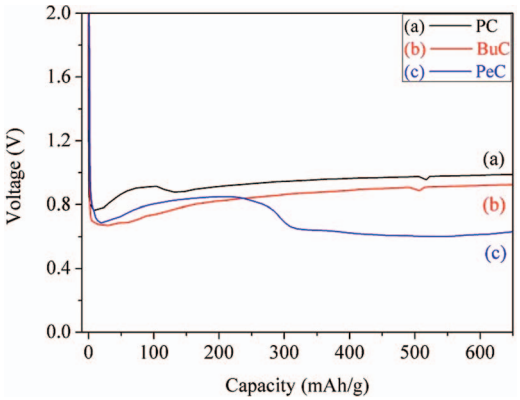

Figure 3. The voltage profiles of graphite-based lithium-ion half cells using (a) PC, (b) BuC and (c) PeC with 1 M $LiPF_6$ at a C/10 rate.

(1.1 V). It is proposed that PeC has the strongest steric hindrance of the three solvents, which needs a larger overpotential for co-intercalation, therefore the cell with PeC-based electrolyte has a plateau with the lowest value (0.6 V).

The solvent decomposition has a destructive effect on the graphite morphology. Figure 4 shows SEM images of graphite electrodes from the three cells, and graphite morphology after cycling in EC/DEC is also shown as a comparison. The morphology in Figure 4b, 4c and 4d shows that the graphite particle isolation and separation cause electrode failure, which was also shown by others.[13,14]

When the cells are cycled in EC/DEC electrolytes, the morphology of graphite surface shows that all the graphite particles are interconnected with each other. However, in the cells showing an exfoliation plateau, graphite particles are electronically separated on the electrode surface. All three cells were cycled for about the same time (∼ 24 h). PC causes dramatic exfoliation over the whole area of the electrode, but the graphite separation by BuC and PeC is less serious.

The physical state of the decomposition products is an important factor to consider whether graphite exfoliation occurs. Based on the proposed decomposition mechanism in Figure 1, the decomposition products expected from various substituted PC solvents are shown in Table II. Propene, 1-butene and 1-pentene are gaseous products with boiling points lower than cycling temperature (30.0°C), which explains why PC, BuC and PeC show the exfoliation behavior when cycled in graphite half cells. 1-hexene, 1-octene and 1-dodecene are non-gaseous compounds, thus, exfoliation does not occur in these solvents.

Bulky solvents prevent graphite exfoliation (HeC, OcC and DoC).— HeC, OcC, and DoC have longer linear alkyl substituents, graphite exfoliation does not occur in these solvents. Moreover, these bulky cyclic carbonates are able to prevent exfoliation when mixed with PC.

The column plot in Figure 5 shows that maximum PC content that the synthesized solvents can tolerate with the increase of carbon numbers on the side chain. With 1 carbon (PC), 2 carbons (BuC) and 3 carbons (PeC), the solvents cause exfoliation of the graphite. With 4 carbons (HeC) in the side chain, HeC is able to prevent exfoliation of the graphite with PC content as high as 20 vol%. When the PC content is higher than 20 percent volume, exfoliation of the graphite takes over. When the side chain length is increased to 6 carbons (OcC) and 10 carbons (DoC), the transition points are 33.3 percent volume and 50 percent volume respectively. It clearly indicates that solvents with a longer side chain and bigger steric hindrance could tolerate more PC content.

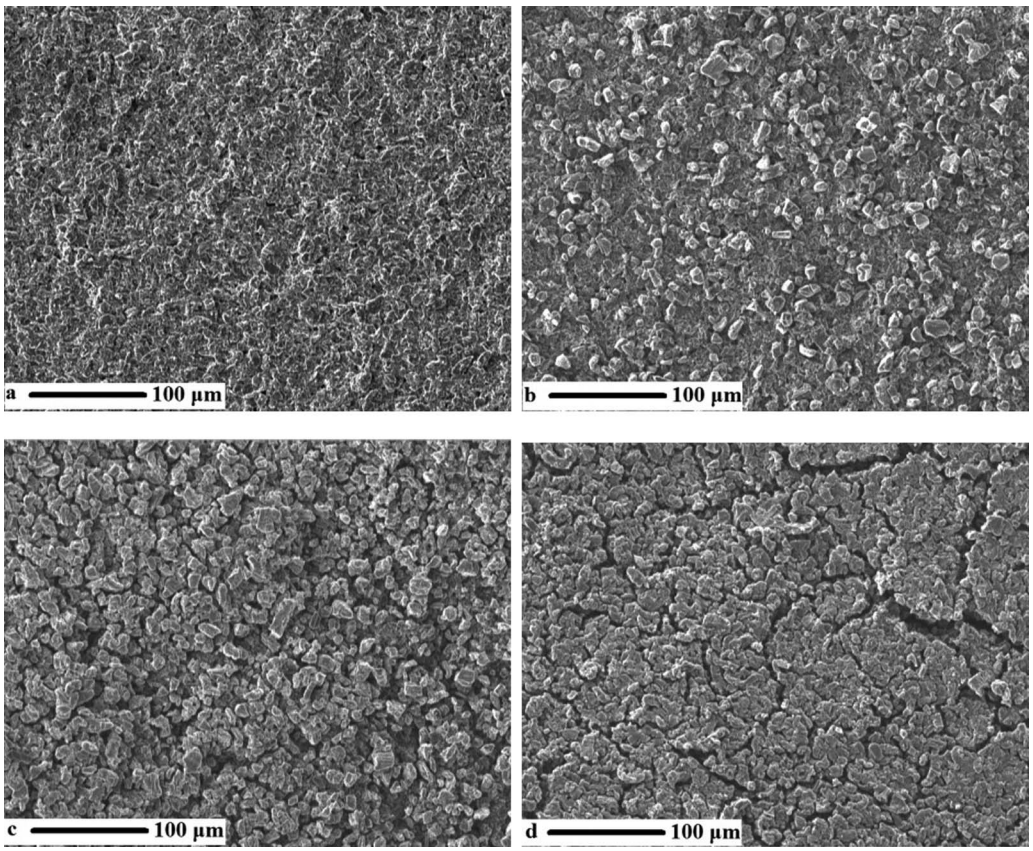

Figure 4. SEM images of graphite anodes after cycling in a 1 M $LiPF_6$ solution of (a) EC/DEC = 1, (b) PC, (c) BuC and (d) PeC at C/10. The scale bar is 100 μm.

Table II. Decomposition products expected from substituted PC solvents from a two-electron reduction mechanism.

Solvent	Decomposition product besides Li_2CO_3	Boiling point of the decomposition product (°C)	Physical state of the decomposition product at cell testing temperature[a]
PC	Propene	−47.6	gas
BuC	1-Butene	−6.3	gas
PeC	1-Petene	30.0	gas
HeC	1-Hexene	63.3	liquid
OcC	1-Octene	121.0	liquid
DoC	1-Dodecene	213.8	liquid

[a]The cells were tested at 30°C.

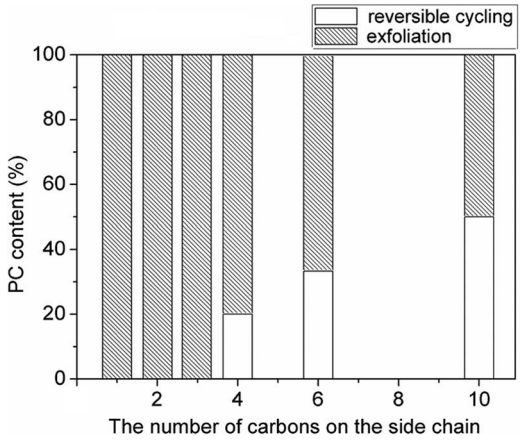

Figure 5. Influence of steric hindrance on the ability to prevent exfoliation.

Figure 6 shows cycling performances of graphite half cells using co-solvents of HeC/PC = 4, OcC/PC = 2, and DoC/PC = 1 with 1 M $LiPF_6$. Cell capacities reach ∼ 310 mAh/g in the first 10 cycles in all the electrolytes. This indicates the formation of a stable SEI on graphite surface that prevents PC exfoliation and allows reversible cycling in graphite anode. The PC co-solvents from different batches of HeC, OcC, and DoC gave the same cell performance, which indicates the reproducibility of data shown in Figure 6. Abe et al. studied co-solvents of PC with dimethyl sulfoxide, dimethoxymethane, diethoxymethane, and 1,2-diethoxyethane.[15] All these solvents are able to compete with PC co-intercalation and prevent exfoliation of the graphite. Zheng et al. observed that PC forms a stable film on a graphite surface when mixed with ionic liquid as solvents in a graphite half cell.[16] Due to a similar competing effect by these synthesized cyclic carbonates, exfoliation of the graphite by PC is prevented. Moreover, the electrolytes based on these bulky cyclic carbonate/PC co-solvents form a stable SEI, graphite half cells cycle at a high capacity value with high efficiency.

Figure 7 shows the voltage curves of a lithium-ion half cell using 1 M $LiPF_6$ in HeC/PC = 4. There is a clear plateau in the 1st cycle discharge (lithiation) curve, which corresponds to the decomposition of electrolyte species, this decomposition contributed to a 75 mAh/g capacity before the curve goes down to lithium intercalation voltage (∼0.25 V). The capacity contributed from lithium intercalation is only 150 mAh/g, which is a similar value to the first cycle charge (delithiation) capacity. From first cycle to tenth cycle there is a steady increase of cell capacity, this value is about 310 mAh/g at the 10th cycle.

Figure 8 shows morphologies of a graphite electrode cycled in bulky cyclic carbonates/PC co-solvents. CGP-G8 particles are well-glued together in all three electrolytes. Table III summarizes the electrochemical results obtained from cells with different solvents. In all cases including EC/DEC electrolytes, there is steady increase of efficiency and capacities. First-cycle efficiencies of graphite half cells based on bulky cyclic carbonate/PC electrolytes are in the range of 70 ∼ 80 percent, which is lower compared to the value in EC/DEC (92 percent). Besides SEI formation, there must be other side reactions that contributed to the low efficiency in the bulky cyclic carbonate/PC electrolytes. Regardless of the initial performances, all these cells reach high efficiencies in the 60th cycle. The efficiency for HeC/PC = 4 electrolyte is around 99.98, which is comparable to the cell based on EC/DEC electrolytes.

Figure 9 shows the 10th cycle potential profiles of graphite half cells using different electrolytes. Cell performances based on a synthesized cyclic carbonates/PC mixture are quite similar to those of EC/DEC-based cells. The embedded figure shows that the impedance from a cell cycled in EC/DEC is the lowest of all four cells. In terms of the three cells with mono-substituted cyclic carbonate/PC co-solvents, the

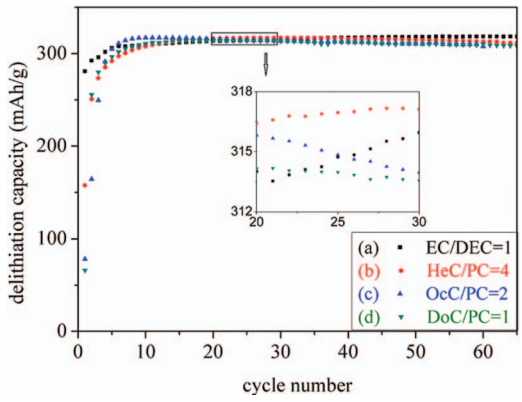

Figure 6. Cycling performances of a graphite half cell in a 1 M $LiPF_6$ solution of (a) EC/DEC = 1, (b) HeC/PC = 4, (c) OcC/PC = 2, and (d) DoC/PC = 1 (v/v) at a C/10 rate.

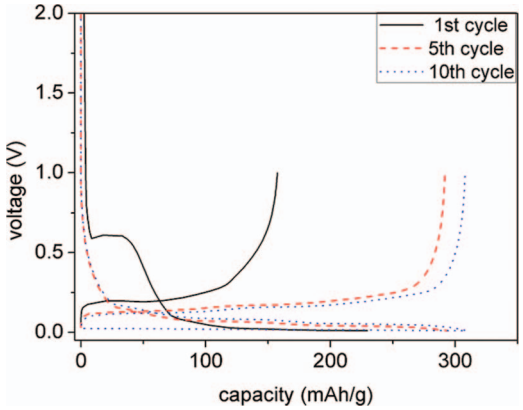

Figure 7. Potential profiles of the 1st, 5th, and 10th cycles for cells cycled with 1 M $LiPF_6$ in HeC/PC = 4.

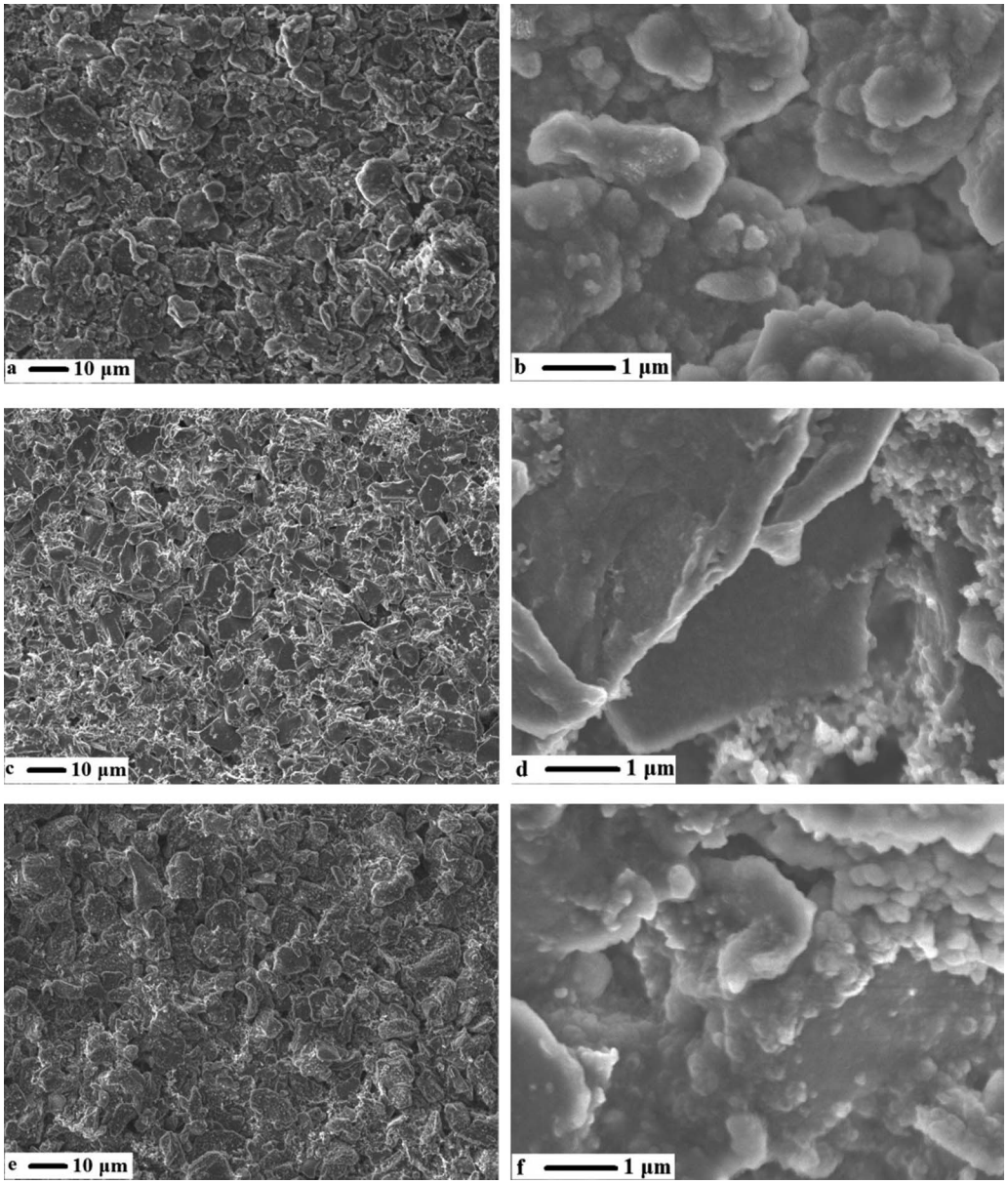

Figure 8. SEM images of graphite anodes after cycling in a 1 M $LiPF_6$ solution of (a) (b) HeC/PC = 4, (c) (d) OcC/PC = 2, and (e) (f) DoC/PC = 1 (v/v) at a C/10 rate for 10 cycles. The scale bars are 10 μm in (a), (c), and (e), and 1 μm in (b), (d), and (f).

Table III. Electrochemical data of the graphite anode in a 1 M $LiPF_6$ solution of different solvents at C/10.

		EC/DEC = 1[a]	HeC/PC = 4[a]	OcC/PC = 2[a]	DoC/PC = 1[a]
1st cycle	Q_c[b] (mAh/g)	279.4	146.5	78.2	65.9
	η[c] (%)	92.20	68.53	78.62	72.13
10th cycle	Q_c[b] (mAh/g)	304.2	309.1	318.3	312.8
	η[c] (%)	99.89	99.64	99.68	99.40
60th cycle	Q_c[b] (mAh/g)	318.4	313.1	307.9	310.4
	η[c] (%)	99.99	99.98	99.82	99.51

[a] volume ratio.
[b] charge (delithiation) capacity.
[c] Coulombic efficiency.

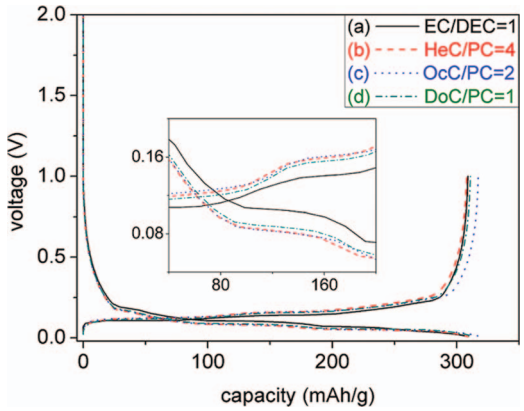

Figure 9. The potential profiles of graphite half cells at the 10th cycle cycled in a 1 M $LiPF_6$ solution of (a) EC/DEC = 1, (b) HeC/PC = 4, (c) OcC/PC = 2, and (d) DoC/PC = 1 (v/v) at a C/10 rate.

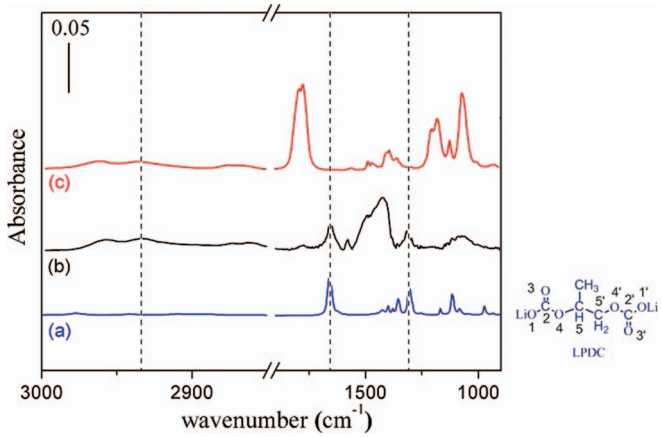

Figure 11. FTIR spectra of (a) a standard LPDC, (b) a graphite electrode cycled in a 1 M $LiPF_6$ solution of HeC/PC = 4 for around 10 cycles at C/10, and (c) the electrolyte used in the cell, 1 M $LiPF_6$ in HeC/PC = 4.

DoC/PC co-solvent gives the lowest impedance, probably because of the higher PC content. Because of the relatively high impedance from this series of PC co-solvents compared to EC/DEC, it may influence their high rate performance. The rate performances of this series of PC co-solvents are shown in Figure S11 in the supporting information, which show a worse performance than EC/DEC electrolyte.

A proposed explanation for the reversible cycling of graphite half cells in these PC co-solvents is shown in Figure 10. When the solvent is HeC/PC = 4, as shown in Figure 10, most of the solvents in the solvated Li^+ are HeC, because of the large ratio of HeC in the electrolyte, the bulky solvent molecule makes it difficult to co-intercalate into the graphene layers. Because of the deficiency of electrons on the graphite surface compared to inside the graphene layers, most PC molecules decompose via a single-electron reduction mechanism. As shown in Figure 10, two PC molecules consume two electrons and decompose to propene and lithium propylene dicarbonate (LPDC). LPDC is a good SEI formation component and precipitates on the graphite surface, forming a stable passivation layer, before a large amount of solvent decomposition occurs, a stable SEI is already formed to protect the graphite anode. Both single-electron and two-electron decomposition mechanisms generate propene gas, whether the solvents decomposition occurs on the surface of the graphite or between grapheme layers determines whether graphite exfoliation occurs. Only PC decomposition product is considered for the SEI formation, since the single-electron reduction products of HeC, OcC and DoC have long alkyl chains (Fig. S12), it is proposed that these products are soluble in the electrolytes and unable to passivate the anode surface. Spahr et al. showed that when a graphite surface is thermally treated to facilitate solvent co-intercalation, even EC could cause graphite exfoliation.[17] In our case, the other decomposition product on a graphite surface is a good SEI formation substance, which prevent significant solvent decomposition before a lot of gaseous products are generated.

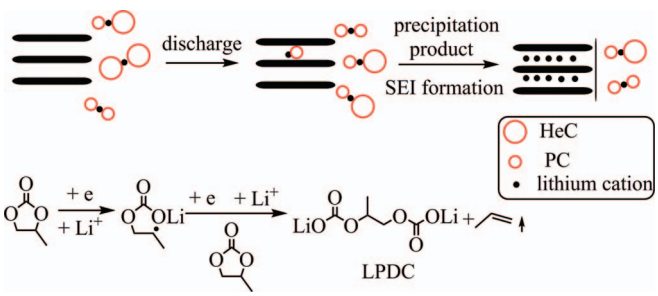

Figure 10. The proposed single-electron reduction path of PC when co-intercalation is delayed by HeC, assuming a solvation number of 2.

Figure 11 shows the FTIR spectra of a graphite electrode after being cycled in HeC/PC = 4 electrolyte. Besides the leftover electrolyte, the major component of SEI is LPDC, which is the single-electron reduction product of PC. A detailed assignment of all the signals in LPDC can be found in literature.[18] The peak at ~ 1660 cm^{-1} is assigned to the carbonyl group O(1)C(2)O(3) in LPDC, which shows up at almost 100 cm^{-1} higher in the cyclic carbonate structure. The vibration mode at 1100 cm^{-1} is assigned to the C(2)O(4)C(5) asymmetric stretching mode. The peak at ~ 1300 cm^{-1} is attributed to the CH_2 wagging mode in the LPDC. The extra broad signal between 1350~1550 cm^{-1} is probably from Li_2CO_3. Although most of the PC goes through single-electron decomposition because of the relative deficiency of electrons on graphite surface, some of the PC may still decompose via a two-electron reduction mechanism, which explains the existence of Li_2CO_3 in the SEI. The signal between 1750~1850 cm^{-1} in curve (c) is assigned to the cyclic carbonate in PC and HeC. Once the solvent decomposes to LPDC, this signal shifts to 1620~1720 cm^{-1}.

Current density also affects the graphite exfoliation in PC.[19] To further explore the influence of cycling rate on the graphite exfoliation behavior, we cycled half cells with HeC/PC = 4 at different rates (C/10 and C/100). Figure 12 shows the results. The cell could reversibly cycle at a 0.1 C rate, but shows exfoliation at a 0.01C rate. The proposed explanation is as follows: at 0.1 C, the solvated Li^+ does not have enough time for co-intercalation, the solvent only decomposes on the surface, as shown in Figure 10. However, when the cycling rate is slow (0.01 C), solvated Li^+ with bulky solvents has enough time to co-intercalate into the graphene layer. The gaseous

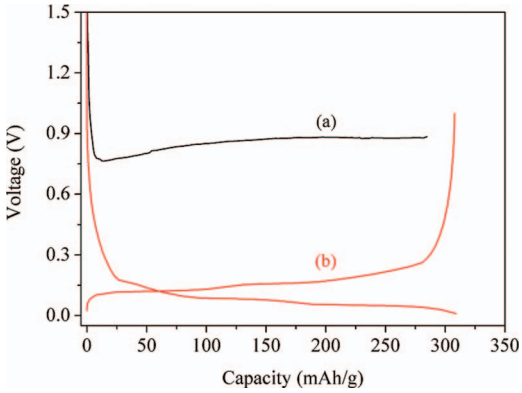

Figure 12. (a) The voltage profile at C/100 and (b) first cycle voltage curve at C/10 in a 1 M $LiPF_6$ solution of HeC/PC = 4 in a graphite half cell.

product (propene) from subsequent decomposition of co-intercalated PC causes graphite exfoliation, as shown in Figure 1. The rate dependence further showcases the influence of steric hindrance on the solvent co-intercalation.

Conclusions

A homologous series of PC derivatives with increasing length of linear alkyl substitutes were synthesized and used as co-solvents in graphite lithium-ion half cells. The synthesized cyclic carbonates with shorter linear alkyl chains (number of carbons $\leqq 3$) decompose to gaseous products once they are co-intercalated into the graphene layers, which induces graphite exfoliation. Cyclic carbonates with longer linear alkyl chains (number of carbons $\geqq 4$) are able to prevent PC exfoliation when mixed with PC. Moreover, graphite half cells with bulky cyclic carbonate/PC co-solvents give a capacity of ~ 310 mAh/g and 99.95 percent efficiency. Further study shows that PC co-intercalation is delayed by the competing solvation of bulky cyclic carbonates. Subsequent single-electron reduction on the graphite surface forms a stable SEI.

Acknowledgments

This work was funded by the Assistant Secretary for Energy Efficiency, Office of Vehicle Technologies of the U.S. Department of Energy (U.S. DOE) under contract no. DE-AC02-05CH 11231 under the Batteries for Advanced Transportation Technologies (BATT) Program.

References

1. M. Winter and J. O. Besenhard, *Lithium Ion Batteries: Fundamentals and Performances*, Wiley-VCH, New York (1999).
2. A. N. Dey and B. P. Sullivan, *J. Electrochem. Soc.*, **117**, 222 (1970).
3. E. Peled, *Lithium Batteries*, Academic Press, New York (1983).
4. J. O. Besenhard, M. Winter, J. Yang, and W. Biberacher, *J. Power Sources*, **54**, 228 (1995).
5. M. D. Levi, N. Levy, S. Sigalov, G. Salitra, D. Aurbach, and J. Maier, *J. Am. Chem. Soc.*, **132**, 13220 (2010).
6. M. R. Wagner, J. H. Albering, K. C. Moeller, J. O. Besenhard, and M. Winter, *Electrochem. Commun.*, **7**, 947 (2005).
7. Y. Yamada, Y. Koyama, T. Abe, and Z. Ogumi, *J. Phys. Chem. C*, **113**, 8948 (2009).
8. A. von Cresce and K. Xu, *Electrochem. Solid St*, **14**, A154 (2011).
9. A. von Wald Cresce, O. Borodin, and K. Xu, *J. Phys. Chem. C*, **116**, 26111 (2012).
10. G. C. Chung, H. J. Kim, S. I. Yu, S. H. Jun, J. w. Choi, and M. H. Kim, *J. Electrochem. Soc.*, **147**, 4391 (2000).
11. G. Liu, H. Zheng, A. S. Simens, A. M. Minor, X. Song, and V. S. Battaglia, *J. Electrochem. Soc.*, **154**, A1129 (2007).
12. R. L. Paddock and S. T. Nguyen, *J. Am. Chem. Soc.*, **123**, 11498 (2001).
13. D. Aurbach, M. D. Levi, E. Levi, and A. Schechter, *J. Phys. Chem. B*, **101**, 2195 (1997).
14. D. Aurbach, H. Teller, and E. Levi *J. Electrochem. Soc.*, **149**, A1255 (2002).
15. T. Abe, N. Kawabata, Y. Mizutani, M. Inaba, and Z. Ogumi, *J. Electrochem. Soc.*, **150**, A257 (2003).
16. H. Zheng, G. Liu, and V. Battaglia, *J. Phys. Chem. C*, **114**, 6182 (2010).
17. M. E. Spahr, T. Palladino, H. Wilhelm, A. Würsig, D. Goers, H. Buqa, M. Holzapfel, and P. Novák, *J. Electrochem. Soc.*, **151**, A1383 (2004).
18. K. Xu, G. V. Zhuang, J. L. Allen, U. Lee, S. S. Zhang, P. N. Ross, and T. R. Jow, *J. Phys. Chem. B*, **110**, 7708 (2006).
19. D. Goers, M. E. Spahr, A. Leone, W. Märkle, and P. Novák, *Electrochim. Acta*, **56**, 3799 (2011).